Mineralogical Magazine, February 2008, Vol. 72(1), pp. 217–220

Transformation of ferrihydrite to hematite: an *in situ* investigation on the kinetics and mechanisms

H. P. Vu*, S. Shaw and L. G. Benning

School of Earth and Environment, University of Leeds, LS2 9JT, UK

ABSTRACT

The kinetics and mechanisms of the transformation of 2-line ferrihydrite (FH) to hematite (HM), in the presence of Pb at elevated temperatures and high pH condition, were elucidated using synchrotron-based, *in situ* energy dispersive X-ray diffraction (EDXRD). The time-resolved diffraction data indicated that HM crystallization occurred via a two-stage process. Based on the EDXRD data, combined with high-resolution electron microscopic images, an aqueous-aided 2D growth mechanism is proposed for both HM crystallization stages.

Introduction

Iron (oxyhydro)oxides (ferrihydrite, FH, hematite, HM and goethite, GT) are ubiquitous and environmentally significant in many terrestrial and marine environments since they control the speciation of many trace elements, including contaminants (Cornell and Schwertmann, 2003). Poorly-ordered ferric oxyhydroxide minerals will tend to transform to more thermodynamically stable minerals (e.g. ferrihydrite (FH) to hematite (HM)). Several studies on the mechanisms of the FH to HM transformation proposed that HM crystallized via an aggregation and recrystallization/dehydration process (Fischer and Schwertmann, 1975; Schwertmann and Murad, 1983). Bao and Koch (1999) used isotopic evidence to confirm this mechanism and showed that water was involved in the crystallization stage. Kinetic studies of HM crystallization from FH suggested that the process was pseudo-first order (Fischer and Schwertmann, 1975; Schwertmann and Murad, 1983; Ford *et al.*, 1999; Shaw *et al.*, 2005).

It has been shown that various metals can affect the stability and crystallization kinetics of FH. Although the transformation of FH in the presence of Pb has been investigated previously (Martínez *et al.*, 1997; Ford *et al.*, 1999), the effect of Pb on the kinetics and mechanisms of this process are still not fully understood. The aim of this study was to investigate the impact of Pb, temperature and pH on the kinetics and mechanisms of FH crystallization under alkaline conditions.

Materials and methods

FH was synthesized following the method of Cornell and Schwertmann (2003). For the transformation experiments, 2 g of freshly precipitated FH were mixed with 15 ml of 1 M NaOH solution and Pb was added immediately from a 21 mM stock solution to reach 20 mg Pb/g FH. The system was equilibrated for 30 min prior to the start of the transformation experiments, which were preformed under isothermal conditions at temperatures between 160 and 240ºC. The crystallization reactions were monitored *in situ* using the time-resolved EDXRD facilities at station 16.4 of the Synchrotron Radiation Source (SRS), Daresbury Laboratory, UK. The details of the station set-up and data treatment were previously described in Shaw *et al.* (2000). Diffraction patterns were collected at 1 min time intervals. The areas under the diffraction peaks for HM and GT were normalized and evaluated using the Johnson-Mehl-Avrami-Kolmogorov model

* E-mail: h.vu@see.leeds.ac.uk
DOI: 10.1180/minmag.2008.072.1.217

(JMAK) (Avrami, 1940) to extract reaction rates and mechanistic information.

Offline experiments preformed at 180ºC (in an equivalent manner to the *in situ* study) were quenched at specific times (after 12, 22, 30, 54 and 100 min, immediately filtered through 0.2 μm polycarbonate filters) and the starting material, all intermediate quenched samples and the end products were characterized by conventional powder X-ray diffraction (XRD, Philips PW1050 X-ray diffractometer, Cu-$K\alpha$), field emission gun scanning electron microscopy (SEM, LEO1530 at 3 keV) and field emission gun transmission electron microscopy (TEM, CM200 working at 197 kV). Finally, the geochemical modelling package *Geochemist's Workbench* (RXN program, version 6.0) was used to evaluate the solubility of HM and GT at the temperatures of interest.

Results and discussion

The time-resolved diffraction patterns indicate a two-stage crystallization process (Fig. 1*a*). In the first stage HM and GT both crystallized from FH, while in the second stage GT transformed to HM. In stage 1, both HM and GT peaks started growing after induction periods (Table 1) while in stage 2 HM peaks continued to grow until they reached a maximum while GT peaks decreased. The evaluated data showing the normalized areas *vs.* time (Fig. 1*b*) confirmed that the transformation occurred in two stages.

Although GT was predicted to form at high pH conditions (e.g. Schwertmann and Murad, 1983; Shaw *et al.*, 2005) the HM observed in this study has recently been reported for other systems reacted at high pH (e.g. Davidson *et al.*, 2008 and references therein). In addition, comparing the solubilities of HM and GT at pH 13 and the temperatures of interest revealed that HM was more stable than GT in all cases (data not shown). It is therefore likely that the high temperatures and the large solid/solution ratio (2 g FH/15 ml solution) in this study favoured the formation of HM over GT. The XRD results from the offline experiments combined with the SEM and TEM images also confirmed the observed two-stage reaction. Interestingly, fitting the decay of GT yielded rates that were similar to the rates of HM growth (Table 1) and thus overall, the data implied that HM crystallized from GT in the second stage.

The kinetic parameters determined from the JMAK fitting include the exponential factor (n), which is related to the reaction mechanism, induction times (t_o) and reaction rates (k) (Table 1). The derived n values were 1 and 2 for the first and the second stages, respectively. An n of 1 for the first stage (pseudo first order) is in agreement with previous studies (Fischer and Schwertmann, 1975; Schwertmann and Murad, 1983; Ford *et al*., 1999; Shaw *et al.*, 2005). For the second stage an n of 2 implies a surface-controlled reaction with a zero nucleation rate (Hulbert, 1969). The derived kinetic parameters (Table 1) are consistent with thermally-activated processes.

The apparent activation energies for nucleation ($Ea_{(nuc.)}$) and crystallization ($Ea_{(cryst.)}$) of HM in both stages were determined from Arrhenius plots (Table 1). The $Ea_{(nuc.)}$ of the first stage is in the range of activation energies for aqueous transport controlled reactions (<21 kJ/mol; Lasaga, 1998)

TABLE 1. Kinetic parameters for growth of HM (110) and decay of GT (110). Errors (2σ) for activation energies (given in parentheses) were calculated by regression statistics.

	Hematite			Goethite
	Stage 1		Stage 2	Stage 2 (decay)
T(ºC)	t_o(s)	k (s^{-1})	k (s^{-1})	k (s^{-1})
160	745	12×10^{-4}	19×10^{-5}	–
180	530	43×10^{-4}	61×10^{-5}	68×10^{-5}
200	418	96×10^{-4}	210×10^{-5}	217×10^{-5}
220	421	123×10^{-4}	332×10^{-5}	312×10^{-5}
240	360	259×10^{-4}	408×10^{-5}	398×10^{-5}
$Ea_{(nuc.)}$ (kJ/mol)		16(±3)	–	–
$Ea_{(cryst.)}$ (kJ/mol)		67(±8)	73 (±11)	–

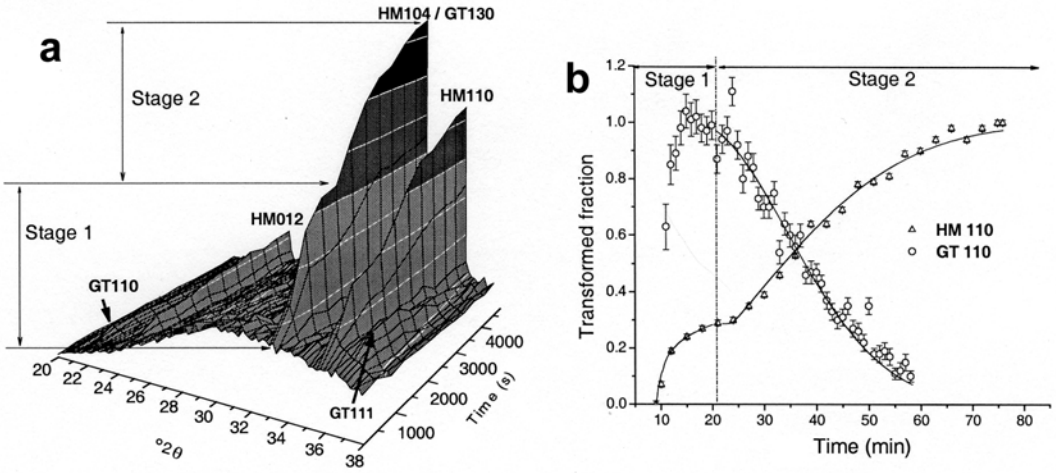

FIG. 1. (*a*) 3-dimensional time-resolved EDXRD patterns; and (*b*) the transformed fraction for the FH to HM and GT transformation at 180ºC. In (*b*) the growth of HM (both stages) and the decay of GT (stage 2) were fitted with the JMAK model.

and is comparable to other published values (Shaw *et al*., 2005, 24(±1) kJ/mol). Previous studies (Fischer and Schwertmann, 1975; Shaw *et al*., 2005) proposed that the nucleation of HM from FH was driven by the aggregation of FH. Thus, it is likely that the formation of HM nuclei in the present study is also a consequence of the aggregation of FH. Previous studies proposed that the crystallization of HM from FH occurred via dehydration – rearrangement processes but with the involvement of local water (Fischer and Schwertmann, 1975; Bao and Kock, 1999). The $Ea_{(cryst.)}$ for the first HM crystallization stage (Table 1) was comparable to a published activation energy (Shaw *et al*., 2005, 69(±6) kJ/mol) and corresponds to an activation energy for a dissolution/precipitation reaction (>34 kJ/mol; Lasaga, 1998). Furthermore, the presence of plate like HM crystals implied that this crystallization stage was controlled by a 2D growth process. Therefore, it can be concluded that in stage 1 HM crystallized via an aqueous-aided 2D growth mechanism. This mechanism agrees well with previous studies (Bao and Koch, 1999; Shaw *et al*., 2005; Davidson *et al*., 2008). However, the presence of Pb in the current study did not alter the mechanisms of the FH to HM transformation.

The $Ea_{(cryst.)}$ of HM crystallization from GT in the second stage (Table 1), is in agreement with a previous high-pH transformation study that also obtained HM as the end product (Davidson *et al*., 2008; 100.3 kJ/mol) and again fits well with values suggested for dissolution/precipitation processes (>34 kJ/mol; Lasaga, 1998). Again this was confirmed by SEM and TEM imaging, which revealed HM associated with GT but showed no evidence supporting a solid-state transformation of GT to HM. It is, therefore, hypothesized that in the second stage HM crystallized from GT via an aqueous-aided 2D surface controlled process with zero nucleation rate.

Conclusion

This study showed that HM formed from FH via a two-stage crystallization process, with GT as an intermediate phase. The data strongly support an aqueous-aided 2D growth mechanism and the results suggest that Pb has little to no effect on the transformation mechanisms but that its presence favoured the formation of HM over GT.

References

Avrami, M. (1940) Kinetics of phase change, II. *Journal of Chemical Physics*, **8**, 212–224.

Bao, H. and Koch, P.L. (1999) Oxygen isotope fractionation in ferric oxide-water systems: low temperature synthesis. *Geochimica et Cosmochimica Acta*, **63**, 599–613.

Cornell, R.M. and Schwertmann, U. (2003) *The Iron Oxides: Structure, Properties, Reactions, Occurrences and Uses*. VCH Verlag, Weinheim. 664 pp.

Davidson, L., Shaw, S. and Benning, L.G. (2008) The kinetics and mechanisms of schwertmannite transformation to goethite and hematite under alkaline conditions. *American Mineralogist*, (in press).

Fischer, W.R. and Schwertmann, U. (1975) The formation of hematite from amorphous iron (III) hydroxide. *Clays and Clay Minerals*, **23**, 33−37.

Ford, R.G., Kemner, K.M. and Bertsch, P.M. (1999). Influence of sorbate-sorbent interactions on the crystallization kinetics of nickel- and lead-ferrihydrite coprecipitates. *Geochimica et Cosmochimica Acta*, **63**, 39−48.

Hulbert, S.F. (1969) Models of solid-state reactions in powder compacts: A review. *Journal of the British Ceramics Society*, **6**, 11−20.

Lasaga, A.C. (1998) *Kinetic Theory in the Earth Sciences*. Princeton University Press, Princeton, New Jersey. 811 pp.

Martínez, C.E., Sauvé, S., Jacobson, A. and Mcbride, M.B. (1999) Thermally induced release of adsorbed Pb upon aging ferrihydrite and soil oxides. *Environmental Science and Technology*, **33**, 2016−2020.

Schwertmann, U. and Murad, E. (1983) Effect of pH on the formation of goethite and hematite from ferrihydrite. *Clays and Clay Minerals*, **31**, 277−284.

Shaw, S., Clark, S.M. and Henderson, C.M.B. (2000) Hydrothermal formation of the calcium silicate hydrates, tobermorite ($Ca_5Si_6O_{16}(OH)_2.4H2O$) and xonotlite ($Ca_6Si_6O_{17}(OH)_2$): an in situ synchrotron study. *Chemical Geology*, **167**, 129−140.

Shaw, S., Pepper, S.E., Bryan, N.D. and Livens, F.R. (2005) The kinetics and mechanisms of goethite and hematite crystallization under alkaline conditions, and in the presence of phosphate. *American Mineralogist*, **90**, 1852−1860.